Measurement, Volume 171, February 2021, Article number 108835
DOI: 10.1016/j.measurement.2020.108835

A Dead Reckoning Localization Method for In-pipe Detector of Water Supply Pipeline: an Application to Leak Localization

Wenming Wang[1 *, 2, 3], Dashan Yang[1], Jifeng Zhang[2], Liyun Lao[3 *], Yuanfang Yin[3], Xiaoxiao Zhu[1]

(1. College of Mechanical and Transportation Engineering, China University of Petroleum-Beijing, Changping, Beijing, 102249, China; 2, Yangtze Delta Region Institute of Tsinghua University, Jiaxing, Zhejiang, 314006, China； 3, Centre for Thermal Energy Systems and Materials, Cranfield University, United Kingdom.)

Corresponding author: Wenming Wang; e-mail: wangwenming@cup.edu.cn;
w.wenmingjob@cranfield.ac.uk.

Abstract: Urban water supply pipeline system integrity is important for the urban life. The aim of study reported in this paper is to locate the water pipeline leak by an in-pipe detector. In this study, a mathematical model is extracted from the actual inspection system. By using the homogeneous transformation theory, transformation matrix which is from carrier to reference coordinate system is deduced, and then the global transformation matrix is obtained to describe the detector's posture. Through measuring the distance increment of each sample time step in carrier coordinate system, the cumulative distance result is calculated. After combining the data of the inertial measurement unit (IMU) and odometer, the leak can be located. To improve the accuracy of leak localization, the magnetic marker is implemented about each 1km distance, which provides reference points which can be used to compensate accumulative error during the localization process. Therefore, a dead reckoning localization method combining data of a micro electro-mechanical IMU, three odometers, and magnetic markers is proposed. To verify above localization algorithm, a simulation case study is conducted with the artificial error generated by the white noise. The simulation results show that the dead reckoning algorithm can effectively provide leak locations with a reasonable uncertainty. Based on this, an experimental platform is built in this study. The experimental results show that the relative error of leak locating achieves a reasonably good performance.

Keywords: in-pipe detector; localization method; water supply pipeline leak; dead reckoning; experiments research.

1 Introduction

Urban water supply is critical and essential infrastructure for the residential and industrial activities. The leak due to damage of water pipeline network could affect people's normal life in the related region, lead to pollution in water supply, and/or risk the underground public facilities. Therefore, various external and internal inspection methods for detecting water supply main pipeline's leak have been developed. The external inspection methods usually rely on the out-pipe sensors which can be conveniently implemented to pick up signals due to leaks [1-2], such as the transient frequency response (TFR) method[3-7], the acoustic emission method, the fiber optic sensing method[8], the magnetic induction method, the ground-penetrating radar method, etc.[9] On the other hand, the internal inspection method, by pushing an in-pipe detector mounting on the detection sensors like hydrophone and pressure transducer into the pipeline section, can sense weak signals as the sensor can be much closer to the location of leaks. The premise is that these pipelines have sufficient diameter to accommodate the detector. In comparing with the external inspection method, it is less sensitive to external noise, and then is easier to detect the small leaking point [10]. It offers a consistent performance along the whole pipeline [11].

A variety of the in-pipe detectors have been reported in the open literatures. Pure Technology Company, developed three in-pipe detectors (the SmartBall, Pipediver, and Sahara), which are able to detect the water leaks as small as 0.02 L/min. They can be launched and retrieved using conventional pig traps [12-13]. The research team at MIT led by Prof. K. Youcef-Toumi designed a number of in-pipe detector prototypes and proposed the methods to differentiate leaks [14-15]. Tianjin University has developed a data acquisition and monitoring system for in-pipe leak inspection and has been applied in the oil pipeline leak check [16-17]. The above system can

effectively detect leaks and achieve high detection accuracy.

The detection principles of internal inspection method based on acoustic signature extraction approaches and pressure gradient analysis in the neighborhood of a leak are usually used [18-19]. It is noted that numerous branches in urban water pipe system which is like leaking conditions to some extent would affect the accuracy of leak detection [20]. However, the branches conditions have no pressure change, which can be distinguished with leak conditions. Moreover, the artificial intelligence diagnose method with traditional sensor is an effective trend to improve the detection accuracy [21-23]. When the leak is discovered, water pipeline maintenance engineering such as mending pipe-wall and replacing old pipeline [19], should be the corrective actions to follow, immediately. Locating the leak points would be essential to perform the pipe repairing operation efficiently.

However, major urban pipelines, particularly those water supply main pipelines, are often buried underground. It means that pipe leak locating is challenging, due to unable to access the global positioning system (GPS) signals during operation process. Apparently lack of an exact leak location will insult in a large area digging, the increasing of pipeline maintenance costs, and even the disturbing of the citizen's life [14]. Therefore, the reliable leak localization is indispensable for the pipeline maintenance project.

Some navigation systems based on the inertial measurement unit (IMU) are proposed to accomplish the localization. However, it should be noted that the IMU has a bias drift problem which leads to the position errors with time [24]. To improve the accuracy, some researchers tried to modify the measurement through adding auxiliary correction instruments such as the weld recognition amending [24-25], the land marker amending [26], the odometer amending [27], etc. Compared with

the signal IMU alignment methods, these methods effectively improve detection accuracy. Huang et al. [24-25] proposed a pipeline orientation method using the magnetic field and acceleration measured simultaneously by the spherical detector. It can accomplish a 3D localization approach for pipelines without any external auxiliary location measurements. Hyun [28] proposed a dead reckoning method for 3D mapping of water supply pipelines. This method uses a micro electro-mechanical IMU and a laser navigation sensor. It can be applied to pipeline mapping and mobile detector positioning. Gong [29] proposed a dynamic precise alignment algorithm based on similar principles. It is proved that the alignment effect based on the map matching result is equivalent to that of single zero error landmark points. Moreover, some researchers tried to decrease the localization error through filtering algorithm. Zhang [30] decreased the error caused by the odometer installation and scale factor error by Kaman filter for the initial navigation system (INS) and odometer system. Huang [31] proposed a Kalman filtering method for odometer-aided inertial navigation system. Experimental results show that the proposed closed-loop method can better estimate the attitude matrix from the current coordinate system to the initial coordinate system.

According to the actual condition of water pipeline, above localization methods can be referred for the design of localization system, and yet they are not suitable to be applied in the water pipeline directly. For instance, comparing literature [24], the water pipeline has not obvious girth welds; optical navigation sensor proposed in literature [28] cannot be applied in the water environment. Therefore, an applicative scheme for the water pipeline is designed, which is low in cost and small in size. Moreover, a multi-sensor fusion algorithm combining the IMU, the odometers, and the magnetic marker is proposed to accomplish the leak localization. To verify the performance of the method, a simulation case and an experimental platform are built, and the error of the localization

system is investigated.

2 System description

The in-pipe detector which consists of support beams, rubber rings, hydrophone, and the dead reckoning localization system is shown in Fig. 1. The size of detector is less than 100mm diameter, which is suitable for the 150mm diameter pipeline. The support beam mounting on the odometer can expand a larger size to contact with inner pipe wall. Moreover, the system can adapt more than 150mm diameter pipe through matching different support beams and rubber rings. When the detector is near the leakage, the pressure gradient descent of fluid is recorded by hydrophone and can determine whether there is a leak [32-33], and then the dead reckoning localization system is used to locate the leak.

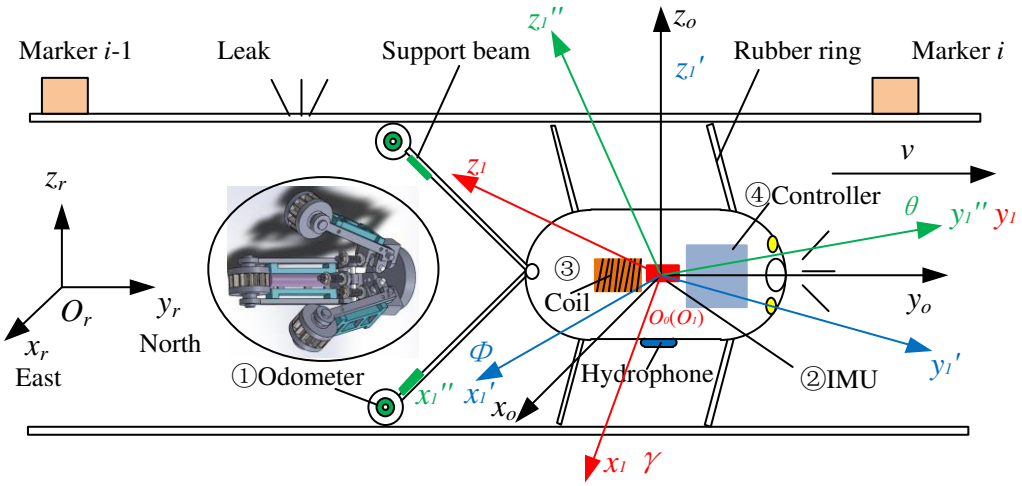

Fig. 1 The scheme of in-pipe detector

The dead reckoning localization system includes three odometers, a micro electro-mechanical IMU, a magnetic marker coil, and a controller unit. The odometers record the moving distance along the pipe axial, and the IMU measures the gyroscope and acceleration of the detector. The leak localization information combining the above moving distance and direction data can be deduced by

the dead reckoning algorithm proposed in section 3. Magnetic marker point is provided every 1km to provide accurate position information of the reference point. The magnetic marker coil can detect the exist markers, and then its position information can be induced to the dead reckoning algorithm to improve the localization accuracy. The correctional localization information can be uploaded to the pipeline geographic information system (GIS) for displaying the leak location. Moreover, the pipe leak need be repaired immediately basing on the localization information.

The controller unit is National Instrument's MyRIO which realizes the signal acquisition, storage and external data transmission. To acquire the navigation data, each odometer wheel records detector's moving distance in every sampling time using the hall sensor NJK-5002 through inspecting the magnetic block; the IMU selects the DY600 sensor which inspects three rotating angles of x, y, z axis and three axial accelerations of detector, and its bias instability is at 1°/h level; magnetic marker coil can detect the land markers of external pipeline, which frequency is 20Hz. The parameters of the sensor are shown in Table 1. The data of the odometers and IMU are measure by frequency 500Hz and 100Hz, and then the data are saved in a TF card. The power supply module uses a large-capacity rechargeable lithium battery pack.

Table 1 Parameters of the detection sensors.

Name	Type	Precise	Sample frequency
IMU	DY600	1° (bias drift 1°/h)	100Hz
Odometer hall sensor	NJK-5002	-	500Hz
Magnetic marker coil	MT-1	0.5m	100Hz

3 Dead reckoning localization algorithm

3.1 Mathematical model

A mathematical localization model of the in-pipe detector is extracted and the coordinate

systems are built as shown in Fig. 2. The reference coordinate system $\{O_r\}$ [34] belonging to the geodetic coordinate system, is established at the starting point: the coordinate origin O_r is the center of detector at starting point; x_r-axis is the east direction, y_r-axis is the north direction, and z_r-axis is the vertical direction. A carrier coordinate system $\{O_0\}$ is established on the center of detector, which is: the coordinate origin O_0 is the detector's center; x_0-axis is vertical to the axial direction of pipeline, y_0-axis is along the axial direction of detector uniformly with that of the pipeline, and z_0-axis is the vertical direction. It is assumed that the starting position of detector is set at t_0 time. The time increment $\Delta t = 0.01s$ is the sampling time of the IMU, and the posture of detector will change along time as shown in the Fig. 2. When the time is t_i, the coordinate system $\{O_i\}$ is described similarly with the coordinate systems $\{O_0\}$.

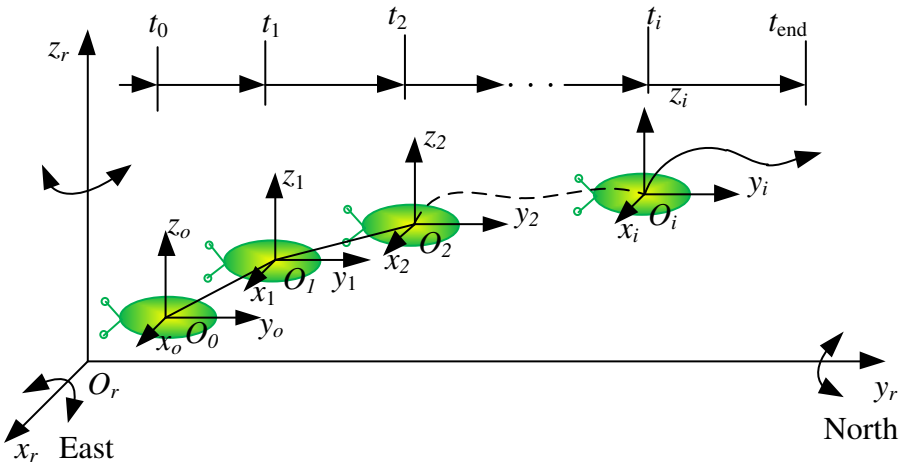

Fig. 2 Mathematic model and trajectory of the in-pipe detector

3.2 Transition matrix

In order to analyze the change of detector position, the movement of detector can be extracted as a vector $\vec{OF}$ in the different coordinate systems as shown in Fig. 3. The vector $\vec{OF}$ is expressed as $\vec{O_rF_r} = \begin{bmatrix} r_{x_r} & r_{y_r} & 0 \end{bmatrix}^T$ in the reference coordinate system $\{O_r\}$, and which is $\vec{O_iF_i} = \begin{bmatrix} r_{x_i} & r_{y_i} & 0 \end{bmatrix}^T$ in the carrier coordinate system $\{O_i\}$.

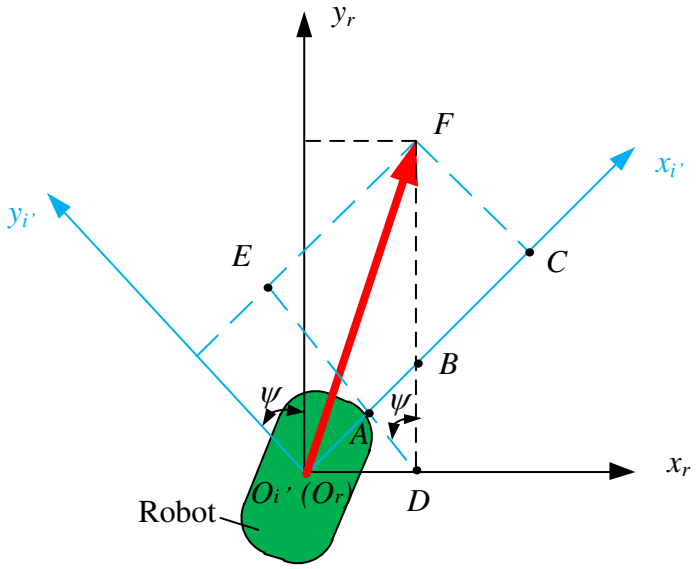

Fig.3 Detector posture using the single-axis transformation.

It is assumed that there is a Ψ of rotation angle around z-axis in $\{O_i\}$, firstly. The coordinate is defined as $\{ r_{xi'}, r_{yi'}, r_{zi'}\}$ which can be represented as Equation (1).

$$\begin{cases} r_{x_{i'}} = r_{x_r}\cos\psi + r_{y_r}\sin\psi \\ r_{y_{i'}} = -r_{x_r}\sin\psi + r_{y_r}\cos\psi \\ r_{z_{i'}} = r_{z_r} \end{cases} \tag{1}$$

After changing Equation (1) into a matrix form, the coordinate transformation matrix from the coordinate system $\{O_r\}$ to $\{O_{i'}\}$ can be obtained as shown in the Equation (2).

$$\begin{bmatrix} r_{x_{i'}} \\ r_{y_{i'}} \\ r_{z_{i'}} \end{bmatrix} = \begin{bmatrix} \cos\psi & \sin\psi & 0 \\ -\sin\psi & \cos\psi & 0 \\ 0 & 0 & 1 \end{bmatrix} \begin{bmatrix} r_{x_r} \\ r_{y_r} \\ r_{z_r} \end{bmatrix} \tag{2}$$

The transformation matrix $T_r^{i'}$ is below.

$$T_r^{i'} = \begin{bmatrix} \cos\Psi & \sin\Psi & 0 \\ -\sin\Psi & \cos\Psi & 0 \\ 0 & 0 & 1 \end{bmatrix} \tag{3}$$

The transformation matrix of $T_r^{i''}$ around x_i-axis and $T_r^{i'''}$ around y_i-axis can be deduced in the

similar way.

$$T_r^{i\prime\prime} = \begin{bmatrix} 1 & 0 & 0 \\ 0 & \cos\theta & \sin\theta \\ 0 & -\sin\theta & \cos\theta \end{bmatrix} \quad (4)$$

$$T_r^{i\prime\prime\prime} = \begin{bmatrix} \cos\gamma & 0 & \sin\gamma \\ 0 & 1 & 0 \\ -\sin\gamma & 0 & \cos\gamma \end{bmatrix} \quad (5)$$

Therefore, the coordinate transformation matrix T_r^i from the reference coordinate system $\{O_r\}$ to the coordinate system $\{O_i\}$ is obtained as shown in Equation (6) [35-36].

$$T_r^i = T_r^{i\prime} T_r^{i\prime\prime} T_r^{i\prime\prime\prime} = \begin{bmatrix} \cos\gamma\cos\Psi + \sin\gamma\sin\Psi\sin\theta & -\cos\gamma\sin\Psi + \sin\gamma\cos\Psi\sin\theta & -\sin\gamma\cos\theta \\ \sin\Psi\cos\theta & \cos\Psi\cos\theta & \sin\theta \\ \sin\gamma\cos\Psi - \cos\gamma\sin\Psi\sin\theta & -\sin\gamma\sin\Psi - \cos\gamma\cos\Psi\sin\theta & \cos\gamma\cos\theta \end{bmatrix} \quad (6)$$

It is noted that T_r^i is the transformation matrix from the reference coordinate system to the carrier coordinate system. To express the matrix in the inverse condition, T_i^r can be obtained as shown in Equation (7) as the transformation matrix between the Cartesian coordinate system is a unit orthogonal matrix.

$$T_i^r = \left(T_r^i\right)^{-1} = \left(T_r^i\right)^T \quad (7)$$

When the angle information of the IMU is input into the Equation (7), the detector posture can be described.

3.3 Mileage calculation

The vector $\vec{OF}$ has the direction and length information. The direction has solved in section 3.2. On the other hand, the length is recorded using the odometer in a sampling time and is calculated by the distance increment ΔS^i in carrier coordinate system $\{O_i\}$ [37]. It can be expressed as shown in the Equation (8).

$$\Delta S^i = \begin{bmatrix} 0 & \Delta S_y^i & 0 \end{bmatrix}^T \tag{8}$$

The distance increment ΔS^i needs to be converted into the reference coordinate system $\{O_r\}$, coordinately. Therefore, the coordinate conversion calculation equation (9) is obtained as follows.

$$\Delta S^{ri} = \begin{bmatrix} \Delta S_x^{ri} & \Delta S_y^{ri} & \Delta S_z^{ri} \end{bmatrix}^T = T_i^r \Delta S^i \tag{9}$$

Where, ΔS^{ri} is the distance increment within time t_i in the reference coordinate system.

To get the position information of the carrier relative to the starting point, it is necessary to accumulate the distance increments from the starting time t_0 to time t_i as shown in the Fig. 2. The cumulative formula is as follows:

$$S_i^r = \begin{bmatrix} x_i \\ y_i \\ z_i \end{bmatrix} = \sum_{j=0}^{i} \Delta S_j^r = \begin{bmatrix} \sum_{j=0}^{i} \Delta S_{xj}^r \\ \sum_{j=0}^{i} \Delta S_{yj}^r \\ \sum_{j=0}^{i} \Delta S_{zj}^r \end{bmatrix} \tag{10}$$

After the cumulative calculation, the position output result (x_i, y_i, z_i) can be obtained, and then the location of detector is realized.

3.4 Magnetic markers correction

To improve the localization accuracy, magnetic markers are deployed along the pipeline to provide an accurate reference position as shown in Fig.4 [38].

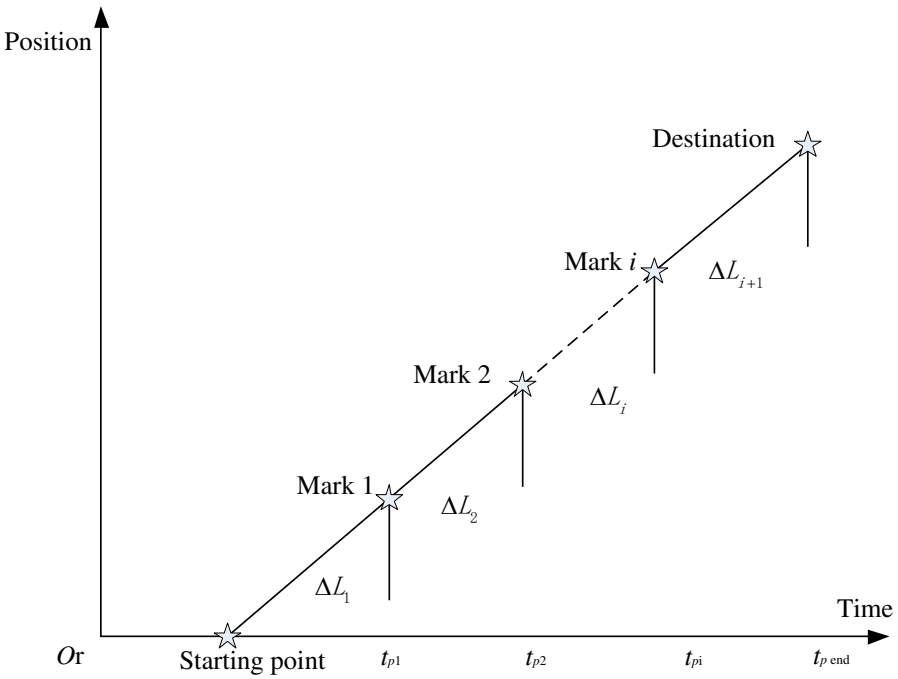

Fig. 4 Magnetic land markers distribution

According to the actual situation of pipeline, magnetic land markers can be layout in the valve well about per 1km and continuously emit low-frequency 20 Hz electromagnetic pulses. When the detector passes through a marker, the magnetic marker coil has a current change response. The marker outside the pipe will be recognized. For example, the position data calculated by the localization system is offset from the actual position is ΔL_i. After passing this location, the coordinate of in-pipe detector become the actual value (x_i, y_i, z_i), and the error would become zero. With the help of magnetic marker information, the positioning accuracy of pipeline can be improved.

4 Simulation

4.1 Examples

To verify the dead reckoning localization algorithm, a simulation case using MATLAB software is conducted as shown in Fig. 5, and the parameters are shown in Table 2 [26]. The simulation trajectory has three phases including two straight sections and an elbow section. The lengths of the

straight section I and II are both 5m, and the angel of the elbow section is 90°. The starting point is A (0, 0, 0), and the destination point is B (-6.1559, 6.1359, 0). The total motion duration is within 24s. In phase I, the movement speed is 0.5m/s until 10s. In phase II, there are a constant velocity of movement of 0.2m/s and a rotation speed of 10°/s around the *z*-axis from 10s to 19s. In phase III, the movement velocity is 1.0m/s from 19s to 24s.

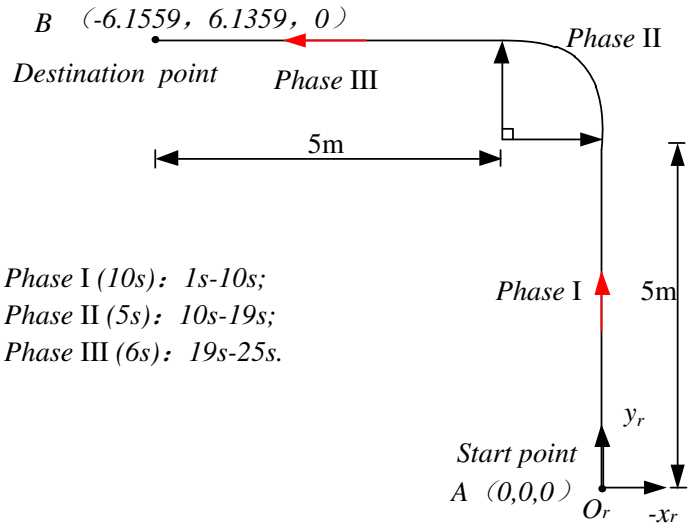

Fig. 5 Trajectory diagram of the simulation case.

Table 2 Simulation motion parameters.

Phase	Time	Time increment (s)	Velocity (m/s)	Rotating speed (°/s)
Phase I	0s-10s	10	0.5	0
Phase II	10s-19s	9	0.2	10° around *z* axis
Phase III	19s-24s	5	1.0	0

It is assumed that the sample frequency of IMU and odometer are both 10 Hz. The simulation data of odometer and gyro are shown in Fig. 6. The curves of ideal data are plotted in Fig. 6 (a). However, under actual circumstances, the data collected has deviation as the sensor error and the measure error. To verify the reliability of the positioning procedure, it is necessary to perform computational simulation of complex data, especially for data simulation with errors. Therefore, white noise of 1‰, 2‰, and 5‰ is introduced to the ideal data, and the data calculation results are

shown in Fig. 6(b), (c), and (d).

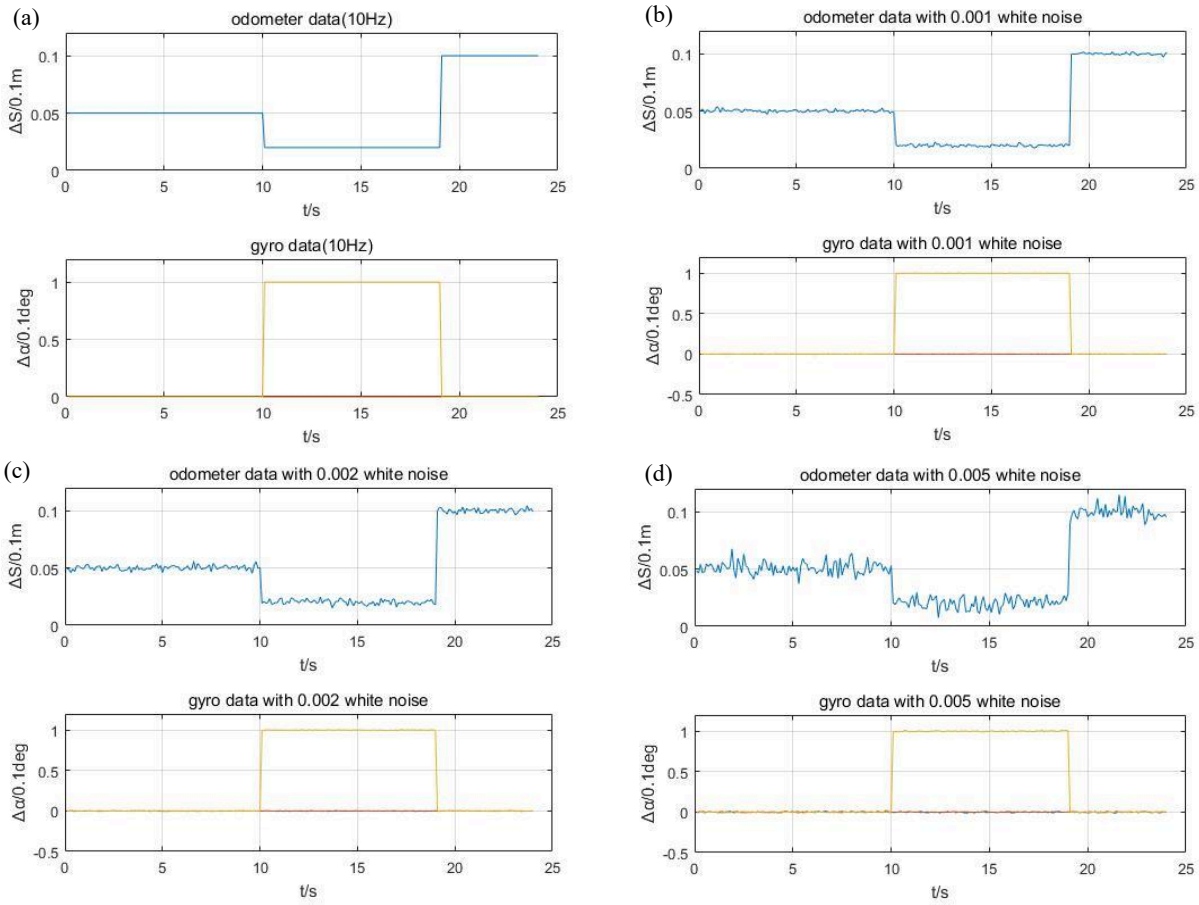

Fig. 6 Simulation data of the odometer and gyro: (a) ideal data; (b) white noise of 1‰; (c) white noise of 2‰; (d) white noise of 5‰.

Fig. 6 shows that there are four values of odometer data and the gyro data, and it has a larger error along the increasing of white noise. Under the white noise of 5‰, the odometer data has a fluctuation of 0.02m/s, and the gyro data has a fluctuation of 0.7°/s.

4.2 Simulation results

The simulation data are imported into the proposed dead reckoning localization algorithm in section 3, and then the results are shown in Fig. 7.

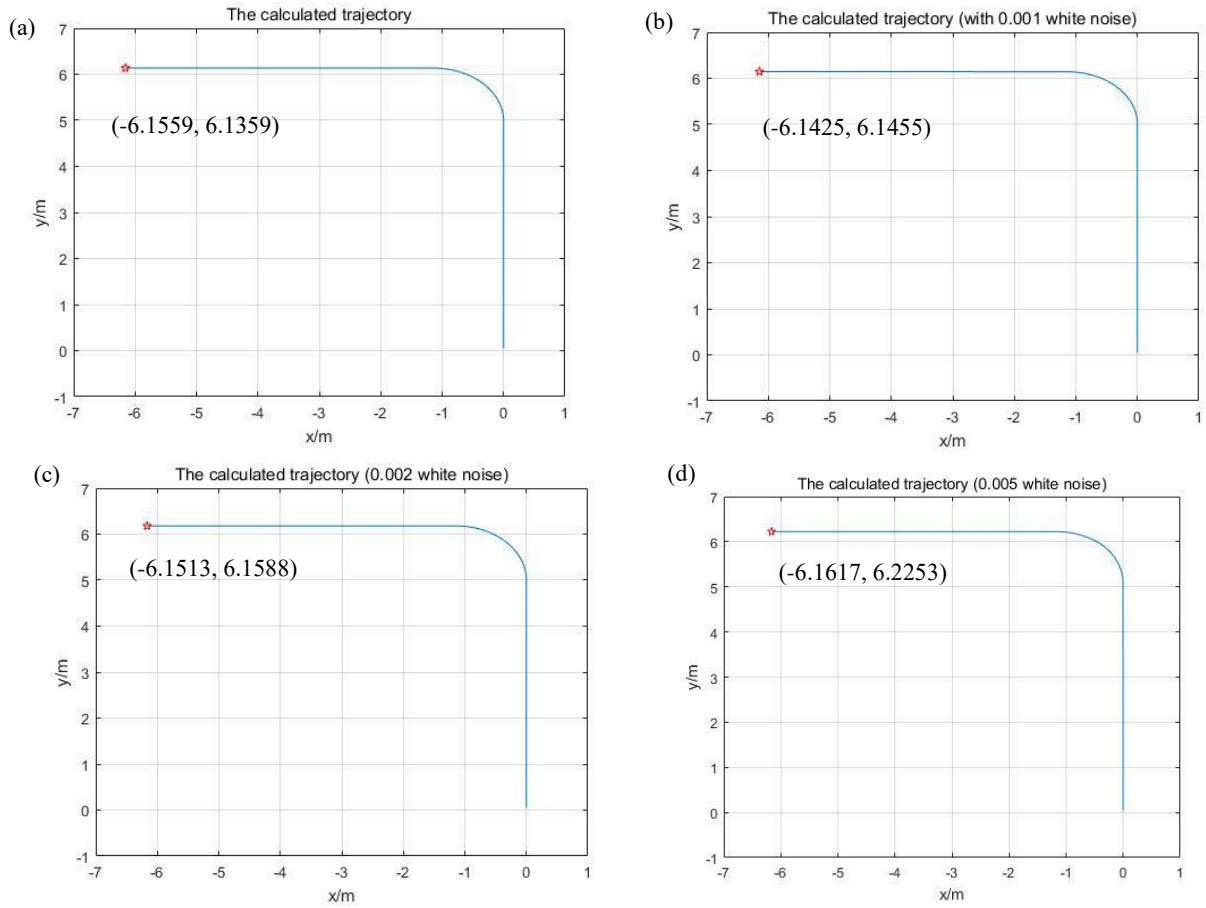

Fig. 7 Simulation result of detector trajectory: (a) the ideal data; (b) white noise of 1‰; (c) white noise of 2‰; (d) white noise of 5‰.

Fig. 7 shows that the calculated displacement curve and trajectory map are consistent with the designed motion. The ideal coordinates of the end position of the motion are (-6.1559, 6.1359). The coordinates of the end point adding the white noisy of 1‰, 2‰, and 5‰ are (-6.1425, 6.1455), (-6.1513, 6.1588), and (-6.1617, 6.2253), respectively. The relative error δ is defined for comparing the calculating results as shown in Equation (11). The error of comparison results are shown in Table 3.

$$\delta = \frac{S - S_r}{S_r} \times 100\% \qquad (11)$$

Where, *S*r is the ideal result; *S* is the white noise result.

Table 3 Comparison of calculation results.

Item	x	y	Relative error (axis x)	Relative error (axis y)	Total maximum error δ
Ideal data	-6.1559	6.1359	-	-	-
White noise of 1‰	-6.1425	6.1455	2.2‰	1.5‰	2.2‰
White noise of 2‰	-6.1513	6.1588	0.7‰	3.7‰	3.7‰
White noise of 5‰	-6.1617	6.2253	0.9‰	14.5‰	14.5‰

The relative error is decided the precision of localization. When the white noise is 1‰, 2‰ and 5‰ of ideal data, the total error δ is 2.2‰, 3.7‰, and 14.5‰, respectively. It is indicating that there is a serious effect from white noise. The positioning algorithm can achieve accurate localization when the white noise is under 2‰. However, the total maximum error is 14.5‰ when the white noise is 5‰. Therefore, to accomplish a precise localization, the high precise sensor need be selected and the filter should be conducted.

5 Experiments and results

5.1 Outside pipe experiment setup

A localization test platform is designed as shown in the Fig. 8 (a). A universal four-wheel robot is used to simulate the in-pipe detector, and its total size is 280mm×150mm×120mm. The localization system including the IMU, odometers, and magnetic marker coil is installed on the robot. The sensors data are sent to NI MyRIO 1900 real-time controller to calculate the localization result. The baud rate between the IMU and controller is 15200bps, and the sampling rate is 100 Hz. Three odometers are mounted on the tail of experimental robot platform, and the sampling rate is 500 Hz. Make sure that an odometer is always in contact with the ground to measure travel distance. The actual test path of localization experiments with a flat ground is conducted around the ‘Petroleum Building’ of China Petroleum University as shown in Fig. 8 (b). The starting point is A, and the

destination point is B. There are three corners in the test, and the total length is 124.20m. The experimental duration time is about 240s, and average velocity of robot is 0.52m/s.

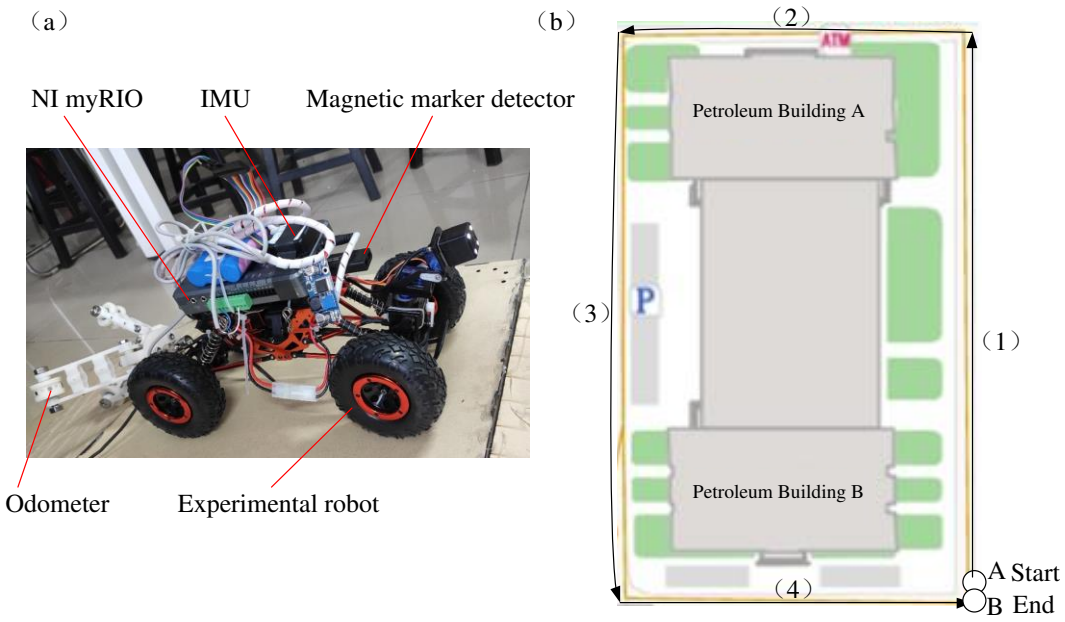

Fig. 8 Experiments: (a) experimental robot; (b) trajectory diagram.

5.2 Outside pipe experimental results

The experimental data are shown in Fig. 9. The rotate angle around axis *x*, *y*, and z are collected by the gyroscope of the IMU. The data of angular velocity around *z*-axis is shown in Fig. 9 (a), and the heading changed angle is shown in Fig. 9 (b). The initial data of odometer is shown in Fig. 9 (c), and the converted displacement is shown in Fig. 9 (d).

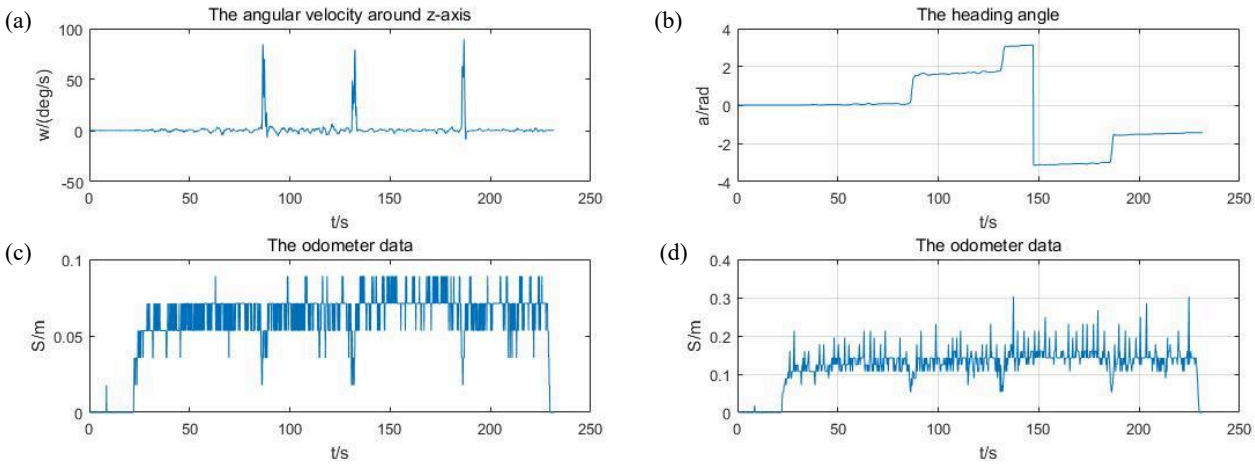

Fig. 9 Experimental data: (a) initial data of the gyro; (b) converted data of the gyro; (c) initial data of the odometer; (d) converted data of the odometer.

The data is calculated using the dead reckoning localization algorithm. Fig. 10(a) and (b) shows the displacement change of *x*-axis and *y*-axis, respectively, and Fig. 10(c) shows the displacement results in the *x*-*y* plane.

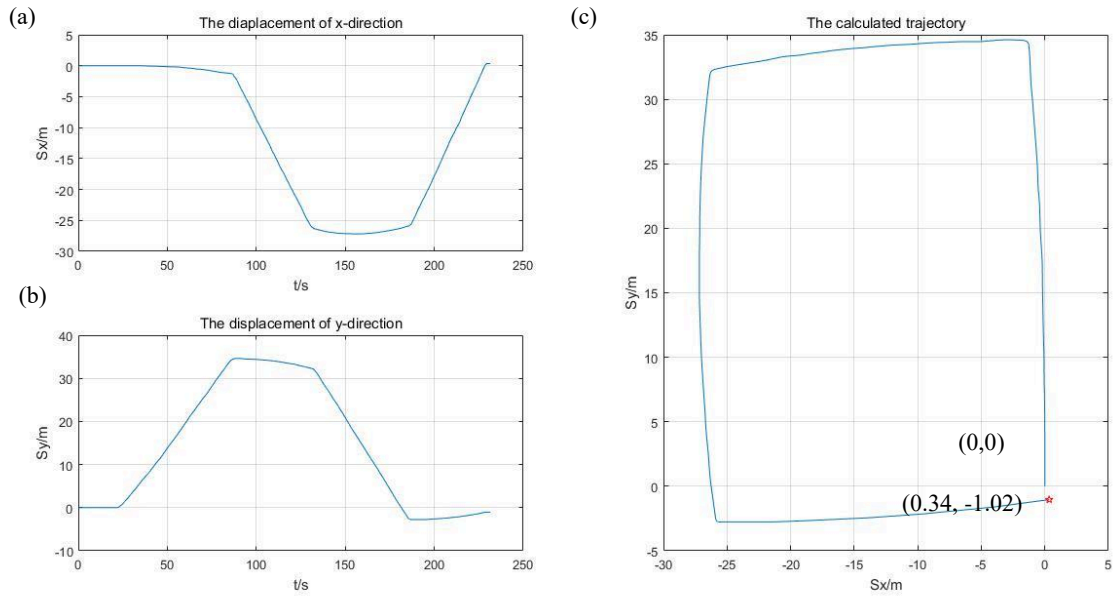

Fig. 10 Experimental results: (a) the displacement curve of *x*-axis; (b) the displacement curve of *y*-axis; (c) the robot trajectory.

Fig. 10(c) shows that calculation robot trajectory is consistent with the actual movement trajectory. The calculated destination position is (0.3422, -1.0302), and the calculation length can be obtain which is 122.90m. Because the total length is 124.20m, the relative error of distance is as following [39]:

$$\delta_l = \frac{122.90 - 124.20}{124.20} \times 100\% = 1.0\% \qquad (12)$$

To verify the dead reckoning algorithm, another 4 experiments are conducted, and the relative errors are shown in Table 4.

Table 4 Comparison of calculation results.

Item	*x*/m	*y*/m	Calculation length (m)	Relative error
Ideal	0	0	124.20	-
1	0.34	-1.02	122.90	1.0%
2	0.51	-0.64	122.59	1.3%
3	0.44	-0.32	123.08	0.9%
4	0.61	-0.91	122.46	1.4%
5	0.52	-0.63	122.59	1.3%

Table 4 shows that relative errors of distance using dead reckoning localization algorithm are within ±1.5%, achieving a reasonably good performance for robot localization in laboratory scale.

5.3 Experimental results of pipeline test loop

A test loop of water pipeline was deployed as shown in the Fig. 11. The diameter of pipeline is 200mm, and the pipeline loop scale is 3.5m×5.5m. An in-pipe detector designed by our laboratory was injected into the pipeline by a launcher to record the distance and direction. The pipeline was filled with water by the water pump. The starting point was A (0,0), and the ideal destination point was B(0,5.50). There were two corners in the test trajectory, and the total length was 10.6m. The experimental duration time was about 180s, and average velocity of in-pipe detector was 0.06m/s.

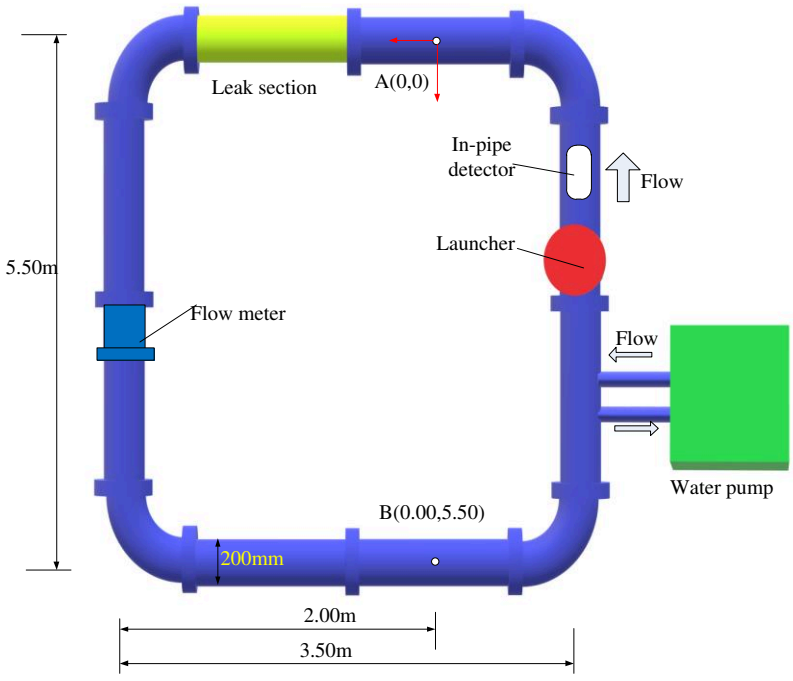

Fig. 11 Experimental pipeline test loop

The data was calculated using the dead reckoning localization algorithm. The experimental results were obtained as show in Table 5, and the distance is 10.47m. The maximum relative error of distance is 1.2% based on equation (12), which shows that relative error also achieves a reasonably good performance in the pipeline test loop.

Table 5 experimental results in test loop.

Item	*x* direction	*y* direction	Calculation length (m)	Relative error
Ideal	0.00	5.50	10.6	-
Experiment results	0.06	5.41	10.47	1.2%

6 Conclusions

In present work, a leak location method based on the dead reckoning algorithm was proposed, and simulation and experiment which verified the location theory was investigated.

According to the principle of integrated navigation, a mathematical model of in-pipe detector was built, and then a dead reckoning method combining odometer, magnetic land marker, and IMU was proposed. The direction and length information of the detector can be calculated, and then the leak point can be localized. After a simulation case was assumed, the maximum error of the calculation results was 3.7‰ within 2‰ of white noise data, which verified of the feasibility of the algorithm. In order to verify the accuracy of localization algorithm, an experimental platform was designed, and then test experiments were conducted. The actual experimental data was collected by the odometer and the IMU sensor. The experimental results of outside pipe and pipeline test loop indicate that the localization algorithm is actually feasible [27].

However, the accuracy needs to be further improved. The accuracy of IMU is 1° now, and it can be selected a higher precision sensor in the further. Moreover, the water pipe features such as

branches, expansions, junctions, bends, pipe scales affect the distance measurement using the odometers [40]. The odometers may have more serious phenomenon of wheel-slip, bounce, idling to decrease the measurement accuracy. To solve the above problem, three odometers can be coupled with each other to reduce the distance errors. In the future, more optimized scheme should be considered to increase the localization accuracy.

Acknowledgement

This work was supported by National Natural Science Foundation of China (No. 51309237) and Science Foundation of China University of Petroleum, Beijing (No. ZX20150082, C201602).

References

[1] Datta S, Sarkar S. A review on different pipeline fault detection methods[J]. Journal of Loss Prevention in the Process Industries. 2016;41:97-106.

[2] Liu Z, Kleiner Y. State of the art review of inspection technologies for condition assessment of water pipes[J]. Measurement. 2013;46(1):1-15.

[3] Duan H-F. Transient frequency response based leak detection in water supply pipeline systems with branched and looped junctions[J]. Journal of Hydroinformatics. 2017;19(1):17-30.

[4] Gong J, Lambert MF, Zecchin AC, Simpson AR. Experimental verification of pipeline frequency response extraction and leak detection using the inverse repeat signal[J]. Journal of Hydraulic Research. 2015;54(2):210-219.

[5] Lee PJ, Vítkovský JP, Lambert MF, Simpson AR, Liggett J. Leak location in pipelines using the impulse response function[J]. Journal of Hydraulic Research. 2010;45(5):643-652.

[6] Duan H-F, Lee PJ, Ghidaoui MS, Tung Y-K. Leak detection in complex series pipelines by using the system frequency response method [J]. Journal of Hydraulic Research. 2011;49(2):213-221.

[7] Duan H-F, Lee PJ, Ghidaoui MS, Tung Y-K. System Response Function–Based Leak Detection in Viscoelastic Pipelines [J]. Journal of Hydraulic Engineering. 2012;138(2):143-153.

[8] Gong J, Png GM, Arkwright JW, Papageorgiou AW, Cook PR, Lambert MF, et al. In-pipe fibre optic pressure sensor array for hydraulic transient measurement with application to leak detection [J]. Measurement. 2018;126:309-317.

[9] Chan TK, Chin CS, Zhong XH. Review of current technologies and proposed intelligent methodologies for water distributed network leakage detection[J]. IEEE Access. 2018;6:78846-67.

[10] Chatzigeorgiou D, Youcef-Toumi K, Ben-Mansour R. Design of a novel in-pipe reliable leak detector[J]. Ieee-ASME Transactions on Mechatronics. 2015;20(2):824-833.

[11] Tur JMM, Garthwaite W. Robotic devices for water main in-pipe inspection: A Survey [J]. Journal of Field Robotics. 2010;27(4):491-508.

[12] Fletcher R, Chandrasekaran M. SmartBall™: A new approach in pipeline leak detection[J]. 2008(48586):117-133.

[13] Riaratnam ST, Chandrasekaran M. Development of an Innovative Free-swimming Device [D]. Arizona State University. 2010.

[14] Chatzigeorgiou D, Youcef-Toumi K, Ben-Mansour R. MIT leak detector: modeling and analysis toward leak-observability[C]. IEEE-ASME Transactions on Mechatronics. 2015;20(5):2391-2402.

[15] Wu Y, Kim K, Henry MF, Youcef-Toumi K. Design of a Leak Sensor for Operating Water Pipe Systems[C]. IEEE International Conference on Intelligent Robots and Systems. 2017:6075-6082.

[16] Li B, Chen S, Zhao W, Guo S, Liu Y, editors. Research on Tiny Leak System for Oil Transmission Pipelines[C]. International Conference on Computer Distributed Control and Intelligent Environmental Monitoring; 2012.

[17] Guo S, Chen S, Huang X. CFD and Experimental Investigations of Drag Force on Spherical Leak Detector in Pipe Flows at High Reynolds Number[J]. Computer modeling in engineering & sciences. 2014.101:59-80.

[18] Chatzigeorgiou D, Youcef-Toumi K, Ben-Mansour R, Ieee. Detection & Estimation Algorithms for In-Pipe Leak Detection. American Control Conference [C]. Proceedings of the American Control Conference. 2014: 5508- 5514.

[19] Xu T, Chen S, Guo S, Huang X, Li J, Zeng Z. A small leakage detection approach for oil pipeline using an inner spherical ball [J]. Process Safety and Environmental Protection. 2018.

[20] Meniconi S, Brunone B, Ferrante M, Massari C. Transient tests for locating and sizing illegal branches in pipe systems[J]. Journal of Hydroinformatics. 2011;13(3):334-345.

[21] Waleed D, Mustafa SH, Mukhopadhyay S, Abdel-Hafez MF, Jaradat MAK, Dias KR, et al. An In-Pipe Leak Detection Robot with a Neural-Network-Based Leak Verification System [J]. IEEE Sensors Journal. 2019;19(3):1153-1165.

[22] Cody RA, Tolson BA, Orchard J. Detecting Leaks in Water Distribution Pipes Using a Deep Auto encoder

and Hydro acoustic Spectrograms[J]. Journal of Computing in Civil Engineering. 2020;34(2).

[23] Bui Quy T, Kim J-M. Leak detection in a gas pipeline using spectral portrait of acoustic emission signals [J]. Measurement. 2020;152.

[24] Huang XJ, Chen SL, Guo SX, Zhao W, Zhang Y, Jin SJ. Analyses and application of the magnetic field at girth welds in pipelines[J]. Measurement Science and Technology. 2013;24(11).

[25] Huang XJ, Chen SL, Guo SX, Xu TS, Ma QL, Jin SJ, et al. A 3D Localization Approach for Subsea Pipelines Using a Spherical Detector. Ieee Sensors Journal [J]. 2017;17(6):1828-1836.

[26] Lee D-H, Moon H, Koo JC, Choi HR. Map building method for urban gas pipelines based on landmark detection [J]. International Journal of Control, Automation and Systems. 2013;11(1):127-135.

[27] Chowdhury MS, Abdel-Hafez MF. Pipeline Inspection Gauge Position Estimation Using Inertial Measurement Unit, Odometer, and a Set of Reference Stations[J]. ASCE-ASME Journal of Risk and Uncertainty in Engineering Systems, Part B: Mechanical Engineering. 2016;2(2).

[28] Dongjun Hyun, Hyun Seok Yang, Hyuk-Sung Park, Hyo-Jun Kim. Dead-reckoning sensor system and tracking algorithm for 3-D pipeline mapping [J]. Mechatronics. 2010 (20) :213–223

[29] Gong BC, He CL, Wang XY, Li X. In-Motion Iterative Fine Alignment Algorithm for On-Board Vehicular Odometer-Aided SINS[J]. Journal of Sensors. 2018.

[30] Zhang P, Hancock CM, Lau L, Roberts GW, de Ligt H. Low-cost IMU and odometer tightly coupled integration with robust kalman filter for underground 3-d pipeline mapping [J]. Measurement. 2019;137: 454-463.

[31] Yulong Huang, Yonggang Zhang, Xiaodong Wang. Kalman-Filtering-Based In-Motion Coarse Alignment for Odometer-Aided SINS [J]. IEEE Transactions on Instrumentation and Measurement, 2017.66(12):3364-3377.

[32] Chatzigeorgiou D, Youcef-Toumi K, Ben-Mansour R, Ieee. Modeling and Analysis of an In-Pipe Robotic Leak Detector[C]. IEEE International Conference on Robotics and Automation ICRA. 2014:3351-3357.

[33] Chatzigeorgiou DM, Ben-Mansour R, Khalifa AE, Youcef-Toumi K. Design and evaluation of an in-pipe leak detection sensing technique based on force transduction [J]. New York: Amer Soc Mechanical Engineers; 2013. p 489-497.

[34] Guan L, Cong X, Sun Y, Gao Y, Iqbal U, Noureldin A. Enhanced MEMS SINS Aided Pipeline Surveying System by Pipeline Junction Detection in Small Diameter Pipeline [J]. IFAC. 2017;50(1):3560-5.

[35] Wang WM, Wang LQ, Wang CD. A novel deepwater structures pose measurement method and experimental study[J]. Measurement. 2012;45(5):1151-1158.

[36] Wang WM, Wang LQ, Wang CD. Deep-sea structure pose measurements error analysis and experimental study [J]. Ocean Engineering. 2013;70:141-148.

[37] Wang X, Song H. The inertial technology based 3-dimensional information measurement system for underground pipeline [J]. Measurement. 2012; 45(3):604-614.

[38] Qi H, Zhang X, Chen H, Ye J. Tracing and localization system for pipeline robot [J]. Mechatronics. 2009;19(1):76-84.

[39] Ben Y, Yang J, Yin D, Li Q. System reset of strapdown INS for pipeline inspection gauge [J]. Ocean Engineering. 2014;88:357-365.

[40] Ayati AH, Haghighi A, Lee PJ. Statistical Review of Major Standpoints in Hydraulic Transient-Based Leak Detection [J]. Journal of Hydraulic Structures. 2019. 5(1):1-26.